Autophagy

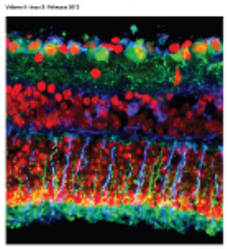

Autophagy

ISSN: 1554-8627 (Print) 1554-8635 (Online) Journal homepage: https://www.tandfonline.com/loi/kaup20

Atg4 recycles inappropriately lipidated Atg8 to promote autophagosome biogenesis

Hitoshi Nakatogawa, Junko Ishii, Eri Asai & Yoshinori Ohsumi

To cite this article: Hitoshi Nakatogawa, Junko Ishii, Eri Asai & Yoshinori Ohsumi (2012) Atg4 recycles inappropriately lipidated Atg8 to promote autophagosome biogenesis, Autophagy, 8:2, 177-186, DOI: 10.4161/auto.8.2.18373

To link to this article: https://doi.org/10.4161/auto.8.2.18373

Autophagy 8:2, 177–186; February 2012; © 2012 Landes Bioscience

Atg4 recycles inappropriately lipidated Atg8 to promote autophagosome biogenesis

Hitoshi Nakatogawa,[1,2,*] Junko Ishii,[1,2] Eri Asai[1] and Yoshinori Ohsumi[1,*]

[1]Frontier Research Center; Tokyo Institute of Technology; Yokohama, Japan; [2]PRESTO; Japan Science and Technology Agency; Saitama, Japan

Keywords: autophagy, cysteine protease, deconjugation, delipidation, lipidation, ubiquitin-like protein

Abbreviations: ALP, alkaline phosphatase; ER, endoplasmic reticulum; PAS, phagophore assembly site/pre-autophagosomal structure; PE, phosphatidylethanolamine

Atg8 is a ubiquitin-like protein required for autophagy in the budding yeast *Saccharomyces cerevisiae*. A ubiquitin-like system mediates the conjugation of the C terminus of Atg8 to the lipid phosphatidylethanolamine (PE), and this conjugate (Atg8–PE) plays a crucial role in autophagosome formation at the phagophore assembly site/pre-autophagosomal structure (PAS). The cysteine protease Atg4 processes the C terminus of newly synthesized Atg8 and also delipidates Atg8 to release the protein from membranes. While the former is a prerequisite for lipidation of Atg8, the significance of the latter in autophagy has remained unclear. Here, we show that autophagosome formation is significantly retarded in cells deficient for Atg4-mediated delipidation of Atg8. We find that Atg8–PE accumulates on various organelle membranes including the vacuole, the endosome and the ER in these cells, which depletes unlipidated Atg8 and thereby attenuates its localization to the PAS. Our results suggest that the Atg8–PE that accumulates on organelle membranes is erroneously produced by lipidation system components independently of the normal autophagic process. It is also suggested that delipidation of Atg8 by Atg4 on different organelle membranes promotes autophagosome formation. Considered together with other results, we propose that Atg4 acts to compensate for the intrinsic defect in the lipidation system; it recycles Atg8–PE generated on inappropriate membranes to maintain a reservoir of unlipidated Atg8 that is required for autophagosome formation at the PAS.

Introduction

The addition of lipid molecules such as myristic acid, palmitic acid and isoprenoides can affect the subcellular localization and function of proteins involved in a wide variety of biological activities.[1-3] Autophagy is a highly conserved, membrane transport system, in which double-membrane bound vesicles called autophagosomes are formed to enclose a portion of the cytoplasm and deliver it to lysosomes or vacuoles for degradation.[4,5] Yeast genetic screens have identified 18 Atg proteins required for autophagosome formation, and a number of studies have revealed their unique features, including that of the ubiquitin-like protein Atg8. A ubiquitin-like system composed of Atg7 (an E1 enzyme), Atg3 (an E2 enzyme) and Atg12–Atg5-Atg16 (a complex with E3 enzyme-like activity) catalyzes amide bond formation between the C-terminal carboxyl group of Atg8 and the amino group in the hydrophilic head of the lipid phosphatidylethanolamine (PE).[6,7] In addition, the cysteine protease Atg4 cleaves the amide bond in the conjugate (Atg8–PE) to release the protein from PE in membranes.[8,9] Thus, the Atg system contains enzymes analogous to those in protein ubiquitination and deubiquitination, and these regulate the lipidation state of Atg8.

We previously showed that in *S. cerevisiae* Atg8 localizes to both forming and complete autophagosomal membranes probably in its PE-modified form.[10] We also showed that Atg8 forms an oligomer when conjugated to PE on liposomes in vitro, leading to the tethering and hemifusion of those membranes, and that this function of Atg8–PE is involved in autophagosome formation in vivo.[11] Most Atg proteins, including Atg8, colocalize at perivacuolar puncta called the phagophore assembly site/pre-autophagosomal structure (PAS), at which they cooperatively act to form autophagosomes.[12] The Atg12–Atg5-Atg16 complex, which is crucial for the lipidation of Atg8, also localizes to the PAS, suggesting that lipidation of Atg8 occurs at the PAS. However, a target membrane for Atg8 lipidation at the PAS still remains to be identified.

In contrast to the lipidation of Atg8, a role for Atg4-mediated delipidation of Atg8 in autophagosome formation remains elusive. A previous study showed that cells defective in Atg8 delipidation exhibit impaired autophagic activity.[8] It has been assumed that delipidation by Atg4 is important for the recycling of Atg8–PE that has fulfilled its role in autophagosome formation. Whereas, in this study, we propose another important role for Atg4 that is required prior to autophagosome formation. As aforementioned,

*Correspondence to: Hitoshi Nakatogawa and Yoshinori Ohsumi; Email: hnakatogawa@iri.titech.ac.jp and yohsumi@iri.titech.ac.jp
Submitted: 02/14/11; Revised: 10/04/11; Accepted: 10/11/11
http://dx.doi.org/10.4161/auto.8.2.18373

it has been thought that the Atg system can restrict the site of Atg8 lipidation to the PAS and produce Atg8–PE at this site in response to autophagy-inducing signals. However, our data suggest that the lipidation system constitutively and nonselectively produces Atg8–PE on various intracellular membranes at considerable frequency. Considered together with other results, we propose that Atg4 functions to compensate for this intrinsic defect in the lipidation system; it recycles Atg8–PE produced on inappropriate membranes to maintain a cytoplasmic pool of unlipidated Atg8 that can undergo lipidation and participate in autophagosome formation at the PAS.

Results and Discussion

Cells unable to undergo Atg8 delipidation are defective in autophagosome formation. In wild-type cells, nitrogen starvation stimulates Atg8 lipidation and induces autophagy (**Fig. 1A**, lanes 1 and 5, and **Fig. 1B**). Atg8–PE is not formed in *atg4*Δ cells, because Atg4 is responsible for both the delipidation and C-terminal processing of Atg8; the latter reaction exposes the glycine residue (G116) of newly-synthesized Atg8, which is essential for its subsequent lipidation (**Fig. 1A**, lanes 3 and 7).[6,8] Therefore, expression of the glycine-exposed form of Atg8 ($Atg8^{G116}$) in an *atg4*Δ strain generates a mutant in which Atg8 can undergo lipidation, but is unable to be delipidated by Atg4. As reported previously, nearly all $Atg8^{G116}$ expressed in *atg4*Δ cells exists as the PE-modified form (**Fig. 1A**, lanes 4 and 8), and these cells show a partial but significant defect in autophagy (**Fig. 1B**). We first examined whether the defect in autophagy was due to reduced autophagosome formation or delayed autophagosome fusion with the vacuole. In *ypt7*Δ cells, which lack a GTPase required for autophagosome-vacuole fusion as well as homotypic vacuole fusion, dots of GFP–Atg8 representing autophagosomes accumulate around fragmented vacuoles under starvation conditions (**Fig. 1C**, upper panels).[10] In contrast, such dots were rarely observed in delipidation-deficient cells (**Fig. 1C**, lower panels). We also performed a protease protection assay to examine autophagosome formation in delipidation-deficient cells. As reported previously,[10] when lysates prepared from *ypt7*Δ cells starved for nitrogen were treated with proteinase K, more than half of the precursor form of Ape1 (pApe1), which was sequestered into autophagosomes, was resistant to the protease but became sensitive in the presence of the detergent Triton X-100 (**Fig. 1D**). Whereas, pApe1 was totally degraded by proteinase K in lysates prepared from *atg1*Δ *ypt7*Δ cells even in the absence of Triton X-100. Thus, the efficiency of autophagosome formation can be assessed with the protease sensitivity of pApe1. In delipidation-deficient *ypt7*Δ cells, protease-resistant pApe1 was significantly reduced compared with *ypt7*Δ cells, suggesting that autophagosomes are less efficiently formed in the absence of Atg8 delipidation (**Fig. 1D**). Moreover, in electron microscopy, autophagosomes (double membrane-bound vesicles with contents identical to the cytoplasm) were less frequently observed in delipidation-deficient *ypt7*Δ cells than *ypt7*Δ cells (**Fig. 1E and F**).[14] Taken together, we concluded that autophagosome formation is impaired in cells unable to delipidate Atg8.

Atg8–PE accumulates on various organelle membranes in delipidation-deficient cells. We noticed that GFP–Atg8 accumulated on fragmented vacuoles in delipidation-deficient *ypt7*Δ cells (**Fig. 1C**). We also examined where Atg8–PE accumulates in delipidation-deficient cells with normal vacuolar morphology (in the presence of Ypt7) (**Fig. 2**). In wild-type cells, a fraction of GFP–Atg8 is sequestered in autophagosomes and transported into vacuoles under starvation conditions, resulting in the GFP staining of the vacuolar lumen (**Fig. 2A**).[10] Consistent with the defective autophagosome formation, the GFP fluorescence inside the vacuole did not significantly increase in delipidation-deficient cells (**Fig. 2A** and **Fig. S1**). We found that GFP–Atg8 localizes to different organelle membranes in the mutant cells. The lipophilic dye FM4–64 stains both vacuoles and endosomes.[15] GFP–Atg8 colocalized with FM4–64 staining in delipidation-deficient cells, suggesting that Atg8 accumulates on both the vacuoles and endosomes (**Fig. 2A**). We confirmed this result using the vacuolar membrane protein Vph1 and the endosomal protein Snf7 as specific markers (**Fig. 2B**). In addition, colocalization with the ER protein Sec63 suggested that Atg8 also accumulates on the ER in the absence of its delipidation (**Fig. 2B**). Disruption of *ATG3* completely abolished the organelle localization of Atg8 in delipidation-deficient cells (**Fig. 3A**), confirming that Atg8 accumulates on these membranes as the PE-modified form.

Atg8–PE accumulation on organelle membranes is independent of the normal autophagic process. We addressed how Atg8–PE accumulates on different organelles in the delipidation mutant cells. First, we showed that the abnormal accumulation of Atg8–PE in the mutant cells was observed even under autophagy-suppressing, nutrient-rich conditions (**Fig. 1A**, lane 4, and **Fig. 2A**). In addition, Atg8–PE still accumulated on organelle membranes in the mutant cells lacking both of the scaffold proteins Atg11 and Atg17 (**Fig. 3A and B**, lane 15), in which all of the Atg proteins fail to localize to the PAS and completely disperse throughout the cytoplasm.[16] These results suggest that the Atg8–PE that accumulates in the mutant cells is produced in a manner independent of the normal autophagic process.

We then examined the involvement of lipidation system components in the accumulation of Atg8–PE in delipidation-deficient cells. The E2 enzyme Atg3 was essential for the production of Atg8–PE in the mutant cells as well as in wild-type cells (**Fig. 3A and B**). In the Atg12–Atg5-Atg16 complex, while the Atg12–Atg5 conjugate directly activates Atg3 to accelerate Atg8 lipidation, Atg16 targets the conjugate to the PAS.[7,16] Thus, the formation of Atg8–PE is impaired in cells defective in this complex (**Fig. 3B**, lanes 5 and 8). We found that deletion of *ATG5* also decreased the accumulation of Atg8–PE in delipidation mutant cells (**Fig. 3A and B**, lane 16), suggesting that Atg12–Atg5 is involved in the production of Atg8–PE in the mutant cells. However, a substantial amount of Atg8–PE was still seen in the mutant cells lacking Atg5, suggesting that basal Atg3 activity also contributes to Atg8–PE production in the mutant cells. Whereas, *ATG16* deletion, which disperses Atg12–Atg5 in the cytoplasm, had no effect on the accumulation of Atg8–PE in delipidation mutant cells (**Fig. 3A and B**, lane 13). In the

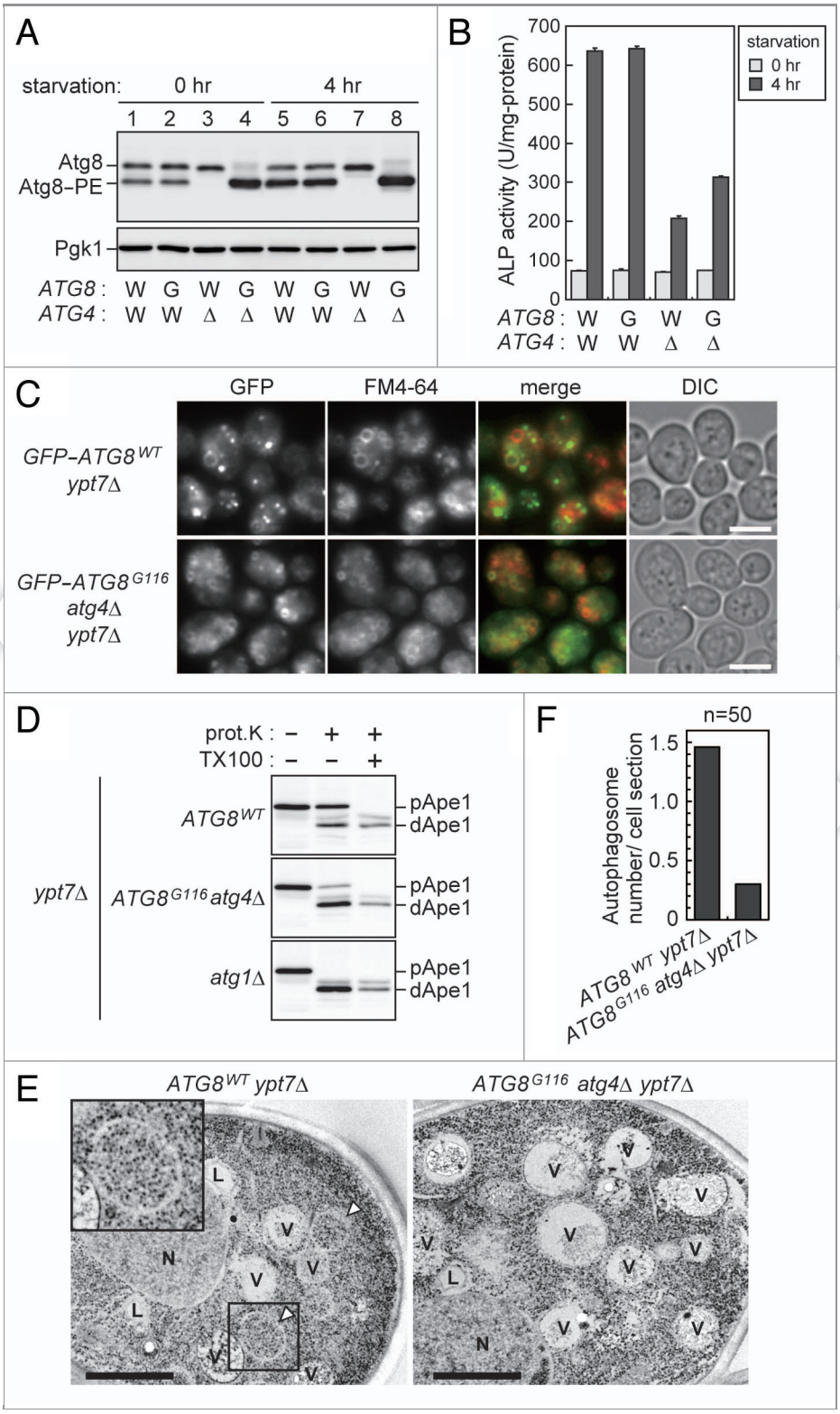

Figure 1. The absence of Atg8 delipidation causes defective autophagosome formation. (A) Yeast strains, YNH490 (wild type), YNH492 (*ATG8*^{G116}), YNH501 (*atg4*Δ), YNH503 (*ATG8*^{G116} *atg4*Δ), were grown to mid-log phase (starvation 0 h) and subjected to nitrogen starvation for 4 h. Lipidation of Atg8 was examined by immunoblotting with anti-Atg8-2 antibodies. It should be noted that these antibodies recognize Atg8–PE with a much higher sensitivity than unlipidated Atg8, similar to anti-Atg8-N and anti-Atg8-IN13 reported previously.[10,11,13] Pgk1 served as a loading control. W, wild type; G, *ATG8*^{G116}; Δ, deletion. (B) These strains were transformed with pTN3, cultured, starved for 4 h, and subjected to the ALP assay to measure their autophagic activities. The experiments were repeated three times, and the means ± standard deviations are shown. (C) YNH448 (*GFP–ATG8*^{WT} *ypt7*Δ) and YNH450 (*GFP–ATG8*^{G116} *atg4*Δ *ypt7*Δ) were labeled with FM4-64 to visualize vacuoles and subjected to nitrogen starvation for 2 h, followed by fluorescence microscopy. Scale bars, 5 μm. (D) YNH448, YNH450, and YNH315 (*atg1*Δ *ypt7*Δ) were grown to mid-log phase and then subjected to nitrogen starvation for 4 h. Cell lysates were prepared from these cells and treated with proteinase K (prot.K) in the presence or absence of Triton X-100 (TX100). These samples were analyzed by immunoblotting with antibodies against Ape1. pApe1, precursor form of Ape1; dApe1, degradation product of Ape1. (E) YNH448 and YNH450 were starved for nitrogen for 4 h and subjected to electron microscopy to examine the accumulation of autophagosomes in the cytoplasm. The arrowheads indicate the autophagosomes. V, vacuole; N, nucleus; L, lipid droplet. Scale bars, 0.5 μm. (F) The number of the autophagosome per cell section was counted (n = 50 for both the strains), and their averages are shown graphically.

presence of Atg16, Atg12–Atg5 localizes to the PAS, but a considerable portion of the complex is also found in the cytoplasm (**Fig. S2**).[16] Taken together, these results suggest that the lipidation system components in the cytoplasm, independently of autophagy, produce the Atg8–PE that accumulates on various organelles in delipidation-deficient cells. Although we could clearly detect Atg8–PE accumulation only on the vacuole, the endosome, and the ER, the lipidation system components in the cytoplasm may mediate Atg8 lipidation on the other intracellular membranes as well. It is also possible that Atg8 lipidation preferentially occurs on certain organelle(s), and Atg8–PE could be redistributed to other organelles via membrane transport systems.

We showed that the absence of Atg4-mediated delipidation did not impair the PAS localization of other Atg proteins, including Atg12–Atg5 (**Fig. S2**; also see below). This excluded the possibility that the altered localization of the Atg proteins caused Atg8–PE accumulation on different organelles in the mutant cells. It is speculated that the diffuse lipidation of

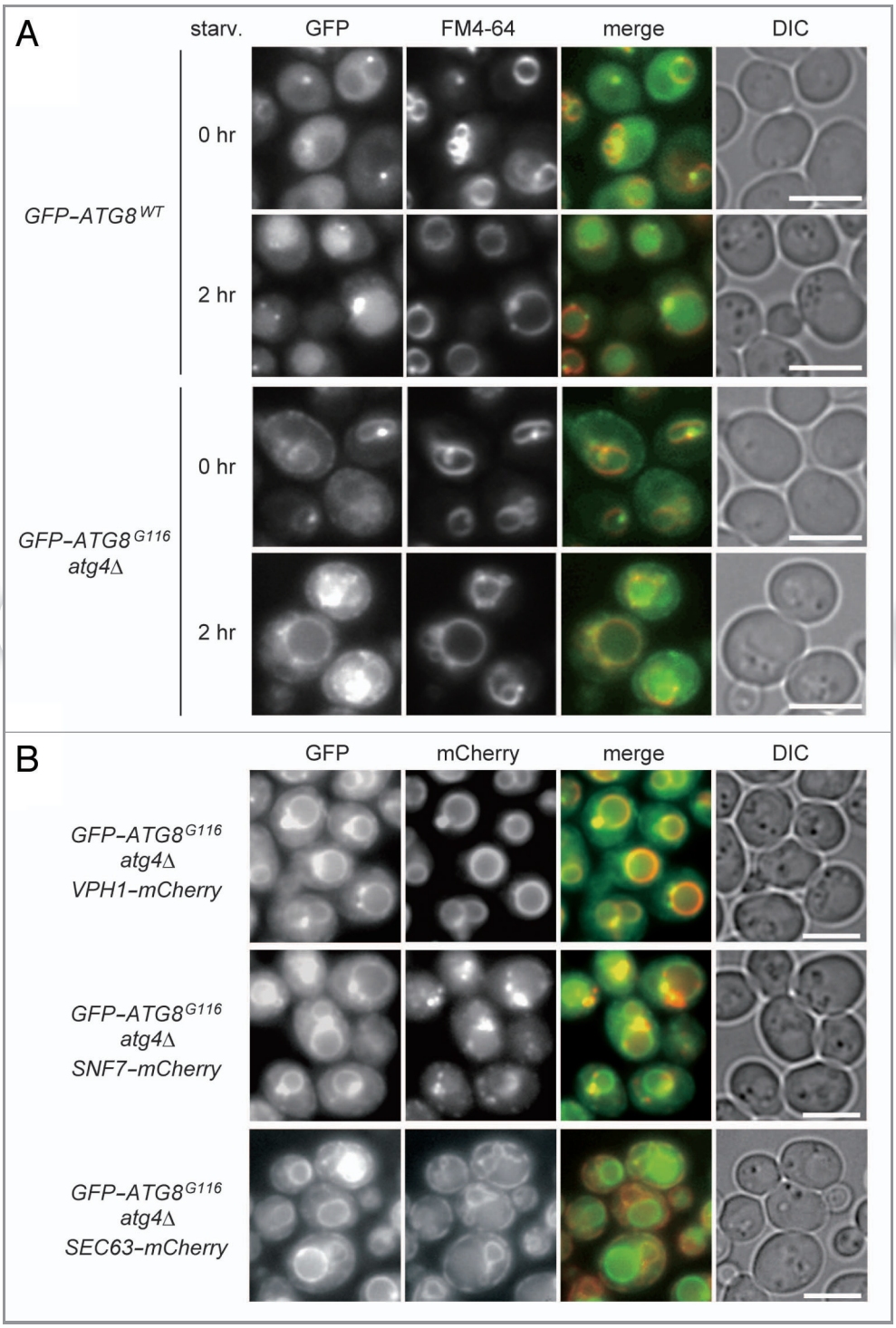

Figure 2. The localization of Atg8 in delipidation-deficient cells. (A) YNH390 (*GFP–ATG8*^{WT}) and YNH442 (*GFP–ATG8*^{G116} *atg4*Δ) were labeled with FM4-64 and observed under a fluorescence microscope before and after 2-h starvation. (B) YNH587 (YNH442, *VPH1–mCherry*), YNH588 (YNH442, *SNF7–mCherry*), and YNH511 (YNH442, *SEC63–mCherry*) were starved for 2 h and examined by fluorescence microscopy. Scale bars, 5 μm.

Atg8 also occurs in wild-type cells, in which Atg8–PE generated on organelle membranes, however, is immediately cleared by Atg4.

A previous study using mutant strains, in which almost all *ATG* genes were deleted and conjugation system components were expressed from plasmids, also suggested that Atg12–Atg5-Atg16 is dispensable for the accumulation of Atg8–PE in the absence of Atg4.[17] In addition, GFP–Atg8 localizes to the rim of the vacuole in a multiple knockout strain expressing Atg7, Atg3 and Atg12–Atg5, but not Atg4.[18]

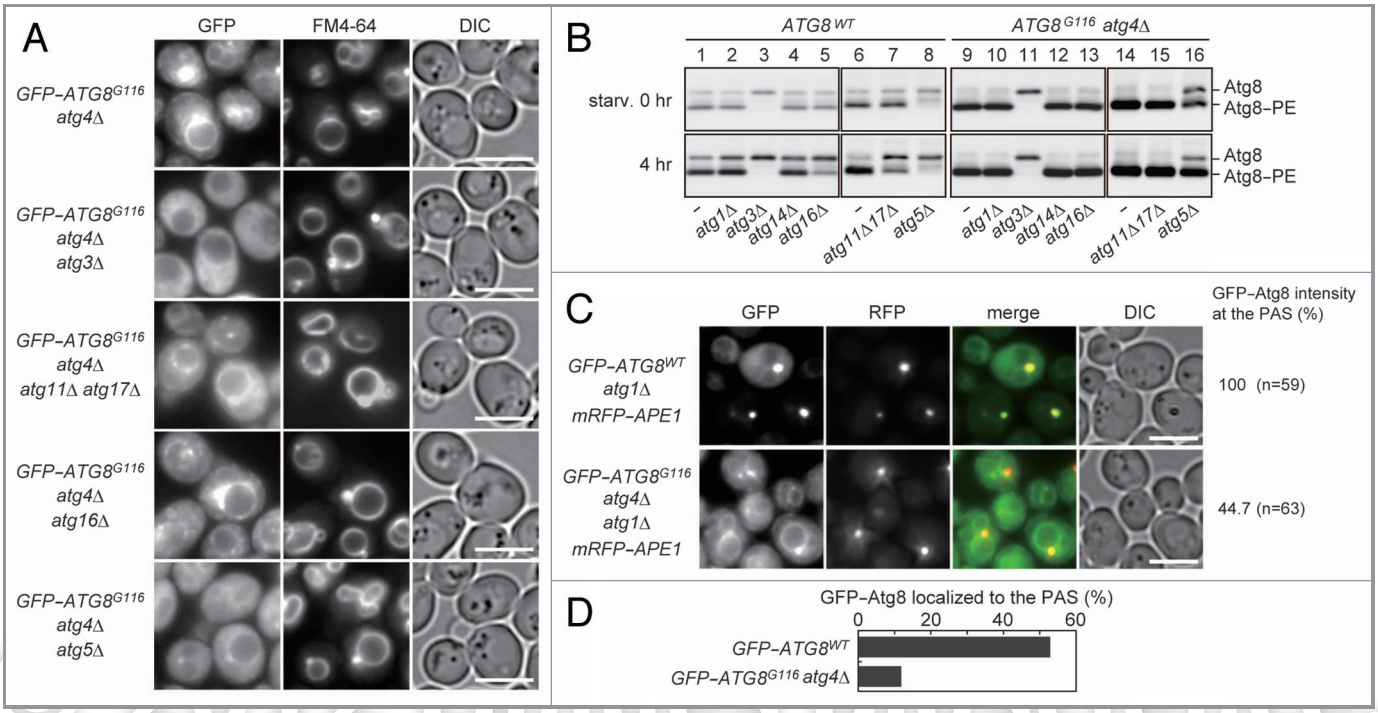

Figure 3. The localization and lipidation of Atg8 in delipidation-deficient cells lacking different *ATG* genes. (A) YNH442 (*GFP–ATG8*^{G116} *atg4*Δ), YNH459 (YNH442, *atg3*Δ), YNH593 (YNH442, *atg11*Δ *atg17*Δ), YNH463 (YNH442, *atg16*Δ), and YNH591 (YNH442, *atg5*Δ) were labeled with FM4-64, subjected to nitrogen starvation for 2 h, and observed under a fluorescence microscope. (B) Lipidation of Atg8 in BY4741 (wild type), YNH204 (*atg1*Δ), YNH208 (*atg3*Δ), YNH214 (*atg14*Δ), YNH332 (*atg16*Δ), YNH258 (*atg11*Δ *atg17*Δ), YNH583 (*atg5*Δ), YNH503 (*ATG8*^{G116} *atg4*Δ), YNH554 (YNH503, *atg1*Δ), YNH555 (YNH503, *atg3*Δ), YNH556 (YNH503, *atg14*Δ), YNH557 (YNH503, *atg16*Δ), YNH586 (YNH503, *atg11*Δ *atg17*Δ), and YNH584 (YNH503, *atg5*Δ) before and after starvation was examined by immunoblotting with anti-Atg8-2 antibodies. (C) YNH662 (*GFP–ATG8*^{WT} *atg1*Δ *mRFP-APE1*) and YNH664 (*GFP–ATG8*^{G116} *atg4*Δ *atg1*Δ *mRFP-APE1*) were starved for 2 h, and the PAS localization of Atg8 in these cells was examined by fluorescence microscopy. The fluorescence intensity of GFP–Atg8 at the PAS (dots of mRFP–Ape1) was quantified, and the average values are shown. Scale bars, 5 μm. (D) YNH661 (*GFP–ATG8*^{WT} *mRFP-APE1*) and YNH663 (*GFP–ATG8*^{G116} *atg4*Δ *mRFP-APE1*) were starved for 2 h, and the PAS localization of Atg8 (the percentage of mRFP–Ape1 dots colocalized with GFP–Atg8) was examined by fluorescence microscopy.

The PAS localization of Atg8 is attenuated in delipidation-deficient cells. Nearly all Atg8 becomes lipidated in the delipidation mutant cells (**Fig. 3B**, lane 9), and it is likely that limited supplies of unlipidated Atg8 cause the defective autophagosome formation in the mutant cells;[19] Atg8 should be recruited to the PAS as the unlipidated form, where lipidated to function in autophagosome formation. In agreement with this notion, the localization of GFP–Atg8 to the PAS, which is observed as a dot adjacent to the vacuole, appeared to be reduced in delipidation-deficient cells. However, the accumulation of GFP–Atg8 at endosomes in the mutant cells obscured the images required for this analysis. To better characterize the PAS localization of GFP–Atg8, we used mRFP–Ape1 as a PAS marker and examined their colocalization in the absence of *ATG1*, which encodes a protein kinase essential for autophagy.[20] We showed that while GFP–Atg8 highly accumulated at the PAS in *atg1*Δ cells,[9,16] this accumulation was reduced in delipidation-deficient *atg1*Δ cells (**Fig. 3C**). We also showed that the frequency of the colocalization of Atg8 with Ape1 significantly decreased in delipidation-deficient cells in the presence of *ATG1* as well (**Fig. 3D**). These results suggest that the PAS localization of Atg8 is attenuated in cells lacking delipidation activity. We also examined the PAS localization of Atg1, Atg14, Atg5 and Atg2, in the delipidation mutant cells (**Fig. S2**). These proteins normally localized to or rather accumulated at the PAS in the mutant cells, suggesting that the impaired PAS localization of Atg8 is not due to the absence of other Atg proteins at the PAS. These results are similar to those obtained when the localization of Atg proteins was assessed in *atg8*Δ cells,[16] and thus consistent with the notion that there is a paucity of Atg8 available at the PAS in delipidation-deficient cells.

Atg4 variants anchored to the vacuole or the ER can support autophagy. While most Atg proteins are known to act at the PAS, the subcellular localization of Atg4 remained uninvestigated. We fused GFP to the C terminus of Atg4 encoded by the chromosomal gene, and performed immunoblotting analysis using antibodies against Atg4 and GFP to show that the fusion protein (Atg4–GFP) was expressed without generating any cleaved product (**Fig. 4A** and data not shown). We also showed that Atg4–GFP is fully functional for autophagy (**Fig. 4B**). Fluorescence microscopy revealed that Atg4–GFP dispersed throughout the cytoplasm and also localized to the nucleus (**Fig. 4C**). We also examined yeast cells expressing both Atg4–GFP and mRFP–Ape1, but their colocalization was not observed (data not shown). The cytoplasmic localization of Atg4 is consistent with the notion that Atg4 can delipidate Atg8 on various intracellular membranes. To gain more insights into the

role of Atg4 in autophagy, we created Atg4 variants that are anchored to vacuolar or ER membranes, where Atg8–PE significantly accumulates in the absence of its delipidation. In *ATG8*^{G116} cells, chromosomally-encoded Atg4 was fused with GFP and sequences derived from the vacuolar membrane protein Nyv1 or the ER membrane protein Cyb5. These variants, Atg4–GFP–Nyv1' and Atg4–GFP–Cyb5', were expressed without any degradation product and localized to the expected organelle membranes (**Fig. 4A and C**). Both the Atg4 variants suppressed the abnormal levels of Atg8–PE accumulation, and maintained the level of unlipidated Atg8 comparable to that seen in wild-type cells (**Fig. 4D**). We also performed density gradient centrifugation analysis to examine where Atg8–PE accumulated in these cells (**Fig. 4E and F**); we could not examine this by fluorescence microscopy because an increased amount of unlipidated GFP–Atg8 in the cytoplasm obscured the localization of the remaining GFP–Atg8–PE. While a small amount of Atg8–PE was found in fractions containing the vacuolar marker Pho8 (fractions 3–5) in cells expressing Atg4–GFP, Atg8–PE that accumulated in delipidation-deficient cells (*ATG8*^{G116} *atg4*Δ) was also distributed in higher density fractions containing the ER marker Dpm1 (fractions 5–10). It was shown that Atg4–GFP–Nyv1' totally suppressed Atg8–PE accumulation even though it was almost exclusively localized to the vacuole (**Fig. 4C**). This Atg4 variant may delipidate Atg8 on not only the vacuole but also the other organelles during its transport to the vacuole via the ER. Whereas, in cells expressing Atg4–GFP–Cyb5', Atg8–PE was significantly reduced in the ER fractions compared with delipidation-deficient cells, although a similar amount of Atg8–PE still accumulated in the vacuole fractions, suggesting that this variant specifically delipidates Atg8 on the ER membrane (**Fig. 4E and F**). The ALP assay showed that autophagy normally occurs in this strain (**Fig. 4B**), suggesting that delipidation of Atg8 on the ER is sufficient to support autophagosome formation. It is conceivable that Atg8 delipidation on the ER can supply a sufficient amount of unlipidated Atg8 that is required for autophagosome formation at the PAS. Alternatively, this may be related to the involvement of the ER membrane in autophagosome formation as proposed by recent studies in mammalian cells,[21-25] although the relation between the ER and the PAS in yeast still remains unclear. Atg4–GFP–Nyv1' was suggested to delipidate Atg8–PE on the vacuole and the other organelles including the ER as well. Cells expressing this variant maintained more unlipidated Atg8 and accordingly showed a higher autophagic activity than cells expressing Atg4–GFP–Cyb5' (**Fig. 4B, D and E**), suggesting that delipidation of Atg8 on the organelles other than the ER also promotes autophagy. We showed that if Atg8^{G116} was additionally expressed from a plasmid in *ATG8*^{G116} *atg4*Δ cells, Atg8–PE further accumulated on organelle membranes, but the autophagic defect was not exacerbated (data not shown). This indicates that the abnormal accumulation of Atg8–PE on organelle membranes is not the cause of the autophagic defect in delipidation-deficient cells and thus that the organelle-targeted Atg4 variants promote autophagic activity by supplying unlipidated Atg8 rather than by eliminating the Atg8–PE that is detrimental to autophagy. Taken together, our results support the notion that autophagosome formation is retarded due to the paucity of unlipidated Atg8 in delipidation-deficient cells and in wild-type cells, cytoplasmic Atg4 recycles Atg8–PE incorrectly produced on different intracellular membranes to maintain a pool of unlipidated Atg8, which is required for autophagosome formation at the PAS.

The results obtained with the Atg4 variants also suggest that the nuclear localization of Atg4 is not important for autophagy, because both Atg4–GFP–Nyv1' and Atg4–GFP–Cyb5', which did not localize to the nucleus, supported normal autophagic activity (**Fig. 4B and C**). The nuclear localization of Atg4–GFP may be an artifact caused by fusion to GFP. It is also possible that Atg4 plays a role independent of autophagy in the nucleus.

PE is a major phospholipid in most biological membranes. Therefore, it is likely that restricting the site of Atg8–PE formation to autophagy-related membranes requires a unique mechanism. It has been thought that the Atg12–Atg5-Atg16 complex localized to the PAS activates the E2 enzyme Atg3 at this site, resulting in the PAS-restricted lipidation of Atg8. However, our data suggest that cytoplasmic fractions of these enzymes erroneously generate Atg8–PE on different organelle membranes to a substantial degree. This depletes the total cellular supply of unlipidated Atg8, which should be recruited to and lipidated at the PAS to be involved in autophagosome formation. Thus, we propose a novel role for Atg4: it releases Atg8 from inappropriate membranes to maintain the level of unlipidated Atg8 sufficient to support autophagy.

Our results are also interpreted as indicating that the existence of Atg4-mediated delipidation allows the localization of the lipidation system components to be loose. Atg proteins are dynamically assembled to and disassembled from the PAS in response to autophagy-inducing signals. In addition, the PAS is located at the perivacuolar region during starvation-induced

Figure 4 (See opposite page). Atg4 constructs engineered to be localized to the vacuole or the ER are functional for autophagy. (A) YNH597 (*ATG8*^{G116} *ATG4–GFP*), YNH503 (*ATG8*^{G116} *atg4*Δ), YNH599 (*ATG8*^{G116} *ATG4–GFP–NYV1'*), and YNH570 (*ATG8*^{G116} *ATG4–GFP–CYB5'*) were analyzed by immunoblotting with anti-Atg4 antibodies. (B) Autophagic activities in these strains carrying pTN3 were determined by the ALP assay. The experiments were repeated three times, and the means ± standard deviations are shown. (C) YNH610 (*ATG8*^{G116} *ATG4–GFP NIC96–TagRFP-T*), YNH612 (*ATG8*^{G116} *ATG4–GFP–NYV1' VPH1–TagRFP-T*), and YNH613 (*ATG8*^{G116} *ATG4–GFP–CYB5' SEC63–TagRFP-T*) were subjected to nitrogen starvation for 2 h and observed under a fluorescence microscope. *NIC96* encodes a nuclear pore complex component. The asterisks indicate the vacuoles visualized by autofluorescence. Scale bars, 5 μm. (D) YNH597, YNH503, YNH599, and YNH570 were examined for Atg8 lipidation before and after starvation by immunoblotting with anti-Atg8-2 antibodies. (E) Cell lysates were prepared from these strains that had been starved for 2 h, and separated by 15–60% OptiPrep density gradient centrifugation. Sixteen fractions were obtained from the top of the gradient, and analyzed by immunoblotting with antibodies against Atg8, Pho8, and Dpm1. (F) The intensities of the bands of Pho8 and Dpm1 shown in (E) were quantified, and their percentages of the total proteins are shown. The band intensities of Atg8–PE were also quantified and are presented, in which the value in fraction 4 in the *ATG4–GFP* strain is set as 100%.

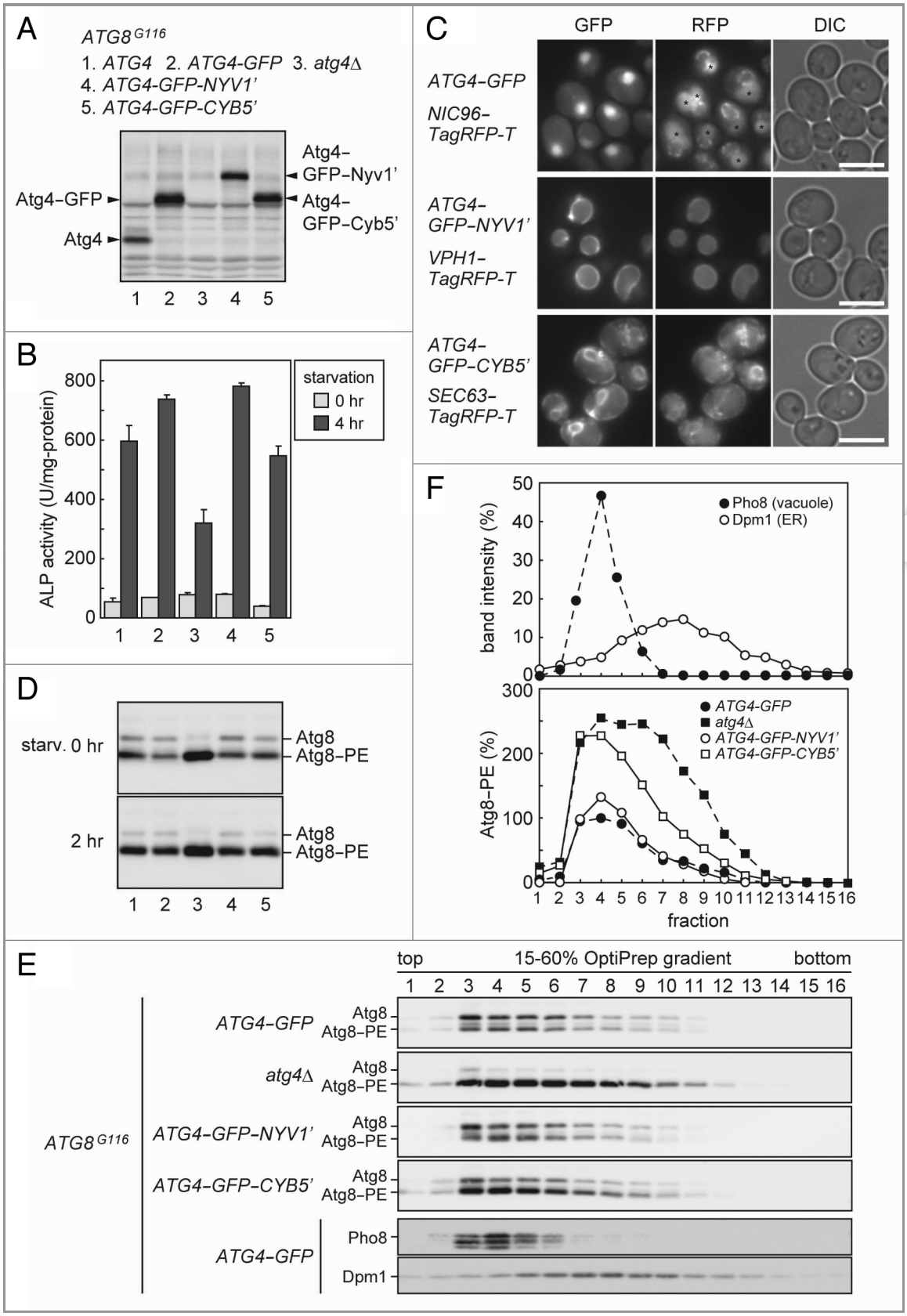

Figure 4. For figure legend, see page 182.

autophagy, but it may need to be organized at other sites; e.g., in the vicinity of mitochondria or peroxisomes during autophagic degradation of these organelles. Therefore, the loose association of the lipidation system components with the PAS and their cytoplasmic fractions may be required to respond to these dynamic features of PAS organization under different situations.

Once generated at the PAS, Atg8–PE must escape delipidation by Atg4 to mediate autophagosome formation. Atg4 may recognize differences in Atg8–PE, e.g., conformation, self-oligomerization, association with other factors, or the curvature of membranes on which the conjugate resides, to prevent its inappropriate delipidation. A structural analysis suggests that the N-terminal tail of Atg4 is involved in this mechanism.[26] It was also proposed that Atg18 and Atg21 may protect Atg8–PE from premature delipidation by Atg4.[18] Alternatively, Atg8–PE may undergo delipidation by Atg4 at the PAS to a similar extent seen on other membranes, but the high levels of Atg8–PE produced at the PAS by the action of Atg12–Atg5-Atg16 exceed its rate of delipidation.

Finally, it should be noted that a novel role for Atg4 we proposed in this study is not mutually exclusive with its previously-proposed role; Atg4 that disperses in the cytoplasm can also recycle Atg8–PE on autophagosomal membranes, which has finished its role in autophagosome formation, as well as Atg8–PE on vacuolar membranes, which has been transferred from the autophagosomal outer membrane upon fusion between these membranes. Further studies are needed to further clarify the mechanism of action of Atg4 in autophagy.

Materials and Methods

Yeast strains and media. All the yeast strains used in this study are derived from BY4741 and listed in **Table S1**.[27] Manipulation of yeast cells was performed using methods described previously.[28] Gene disruption and C-terminal tagging of proteins with fluorescent proteins were performed by a PCR-based method,[29] in which pFA6a-*zeoNT3*, pFA6a-*EGFP-kanMX6*, pFA6a-*mCherry-kanMX6* and pFA6a-*TagRFP-T-natNT2* were used for gene disruption with a zeocin-resistant gene cassette and protein tagging with EGFP and red fluorescent protein derivatives (mCherry and TagRFP-T). To construct strains expressing EGFP–Atg8^{WT} and EGFP–Atg8^{G116}, DNA fragments were amplified by PCR using the plasmids pFA6a-*ATG8p-EGFP–ATG8^{WT}/ATG8^{G116}-ATG8ter-hphNT1* as templates and GFP–ATG8-integ-Fw and -Rv as primers (**Table S2**). Amplified fragments were introduced into yeast cells to allow replacement of the chromosomal *ATG8* gene by homologous recombination. Genomic DNA was isolated from hygromycin-resistant transformants, a region encompassing the *ATG8* gene locus was amplified by PCR, and subjected to DNA sequencing. The resulting strains express EGFP–Atg8^{WT} and EGFP–Atg8^{G116} from the original chromosomal locus with the original promoter and terminator. The strains expressing Atg8^{G116} were similarly constructed with a PCR product prepared using pFA6a-*PGKter-kanMX6* and the oligo DNA ATG8^{G116}-const-Fw and -Rv (**Table S2**). In the resulting strains, transcription of *ATG8^{G116}* is terminated with the *PGK1* terminator, likely leading to increased expression. Therefore, we also constructed strains expressing wild-type *ATG8* with the *PGK1* terminator using the primer ATG8^{WT}-const-Rv, and used these as wild-type *ATG8* control strains. All the pFA6a plasmids described above were donated by Dr. Hayashi Yamamoto. To construct the strains expressing mRFP–Ape1, pPS129 was integrated into the chromosomal *APE1* locus as described previously.[30] The strains expressing Atg4–EGFP–Nyv1' and Atg4–EGFP–Cyb5' were constructed as follows: DNA sequences encoding Asn5 to Trp253 of Nyv1 and Ser92 to Glu120 of Cyb5 were amplified by PCR using genomic DNA from BY4741 as a template and appropriate DNA primers containing a BamHI site at the 5' ends, digested with BamHI, and inserted into the same site in pFA6a-*EGFP-kanMX6*. The resulting plasmids pFA6a-*EGFP–NYV1'-kanMX6* and pFA6a-*EGFP–CYB5'-kanMX6* were used for the C-terminal tagging of Atg4 with EGFP–Nyv1' and EGFP–Cyb5' in combination with the primers ATG4–EGFP–X-Fw and -Rv (**Table S2**). Yeast cells were cultured in SD+CA+ATU media (0.17% yeast nitrogen base without amino acids and ammonium sulfate, 0.5% ammonium sulfate, 0.5% casamino acid, 0.002% adenine sulfate, 0.002% tryptophan, 0.002% uracil and 2% glucose) at 30°C, except that cells carrying pTN3 were cultured in the same media without uracil. To induce autophagy by nitrogen starvation, cells were incubated in SD-N media (0.17% yeast nitrogen base without amino acids and ammonium sulfate and 2% glucose) at 30°C for the indicated time periods.

Immunoblotting analysis. The samples for immunoblotting analysis were prepared by an alkaline extraction method as described previously.[11] Urea-containing SDS-PAGE was performed to separate Atg8–PE from its unlipidated form.[11] Rabbit polyclonal antisera against Atg8 (anti-Atg8-2) and Atg4 (anti-Atg4 #1-2), which were generated using recombinant Atg8^{G116} and Atg4 proteins, were donated from Drs. Yukiko Kabeya and Kuninori Suzuki, respectively. Antibodies against Pgk1 (459250), Pho8 (459260) and Dpm1 (A6429) were purchased from Invitrogen.

Autophagic activity measurement. The autophagic activity of yeast cells was biochemically determined using an alkaline phosphatase (ALP) assay described previously.[31] In this assay, Pho8Δ60, which is a mutant form of vacuolar ALP, is expressed in the cytoplasm as an inactive form. If autophagy occurs, Pho8Δ60 is delivered into the vacuole as a part of the cytoplasm, where it becomes activated. The ALP activity in cell lysates is measured using a fluorogenic substrate. In this study, the plasmid pTN3 was used for Pho8Δ60 overexpression.

Fluorescence microscopy. Fluorescence microscopy was performed using the IX71 total internal reflection fluorescence microscopy system (Olympus), equipped with differential interference contrast optics, a 150 × oil objective lens (Olympus, UApo N 150 × , numerical aperture: 1.45), an electron-multiplying charge-coupled-device camera (Hamamatsu Photonics, ImagEM Enhanced), blue (Coherent, Sapphire 488-20) and yellow lasers (Melles Griot, 85-YCA-010), and bandpass filters (Semrock, FF495-Em02-25 and FF593-Em02-25) for visualization of EGFP and FM4-64/mCherry/mRFP/TagRFP-T, respectively. In the simultaneous observation of these fluorochromes, the lasers were combined, and fluorescence obtained was split into two channels

equipped with the bandpass filters described above, and imaged on different parts of the camera. Images were acquired using Aquacosmos software (Hamamatsu Photonics) and processed using MetaMorph 7.0r4 (Molecular Devices) and Adobe Photoshop CS2.

To visualize vacuoles and endosomes, cells were grown in SD+CA+ATU media to early-log phase, treated with 0.2 μg/ml FM4-64 (Invitrogen, T3166) for 30 min, washed, and incubated in the same media for 30 min. These cells were subjected to nitrogen starvation as indicated, followed by fluorescence microscopy.

Protease protection assay. Yeast cells were grown to mid-log phase and starved in SD-N media for 4 h. 60 OD_{600} units of the cells were harvested, suspended in 5 ml of 0.1 M Tris-HCl (pH 8.0) containing 10 mM dithiothreitol, and immediately resedimented. These cells were suspended in 5 ml of 0.5× SD-N containing 1 M sorbitol and 25 units/ml Zymolyase 100T (Seikagaku Biobusiness, 120493) and incubated at 30°C for 45 min to be converted to spheroplasts. The spheroplasts were washed with 20 ml of ice-cold buffer A [20 mM HEPES-KOH (pH 7.2), 1.0 M sorbitol] twice, gently suspended in 3 ml of buffer A containing 0.5× Complete protease inhibitor cocktail, EDTA-free (PIC) (Roche, 05 056 489 001), and immediately disrupted by passing the suspension through 3 μm-pore-sized polycarbonate membranes (Whatman, 110612). After centrifugation at 500 *g* for 5 min, aliquots of the supernatants were treated with or without 0.2 mg/ml proteinase K (Roche, 3 115 879) in the presence or absence of 2% Triton X-100 on ice for 30 min. The samples were treated with 0.1 M phenylmethylsulfonyl fluoride, followed by trichloroacetic acid (TCA) precipitation. The pellets were washed with acetone, dried and dissolved in the sample buffer for SDS-PAGE.

Electron microscopy. Yeast cells were starved in SD-N media for 4 h and harvested by centrifugation at 2,000 *g* for 2 min, and the pelleted cells were immediately subjected to rapid freezing, freeze-substitution fixation, and electron microscopy performed by Tokai EMA, Inc. based on the methods described previously.[10]

Density gradient centrifugation analysis. Yeast cell lysates were prepared as described above excepting that buffer B [20 mM HEPES-KOH (pH7.2), 0.2 M sorbitol, 5 mM EDTA, 10 mM pefabloc (Roche, 11 429 876 001), 20 mM *N*-ethylmaleimide (NEM), 4× PIC] was used in cell disruption. Nine hundred microliters of the lysates were layered on 10 ml of a 15–60% OptiPrep (Axis-Shield, 1114542) linear gradient prepared using buffer C [20 mM HEPES-KOH (pH7.2), 0.2 M sorbitol, 5 mM EDTA, 5 mM pefabloc, 10 mM NEM, 2× PIC] and centrifuged at 150,000 *g* for 16 h at 4°C. The samples were divided into 16 fractions from the top of the gradients, followed by TCA precipitation for SDS-PAGE sample preparation.

Disclosure of Potential Conflicts of Interest

No potential conflicts of interest were disclosed.

Acknowledgments

We thank Dr. Daniel Klionsky for providing the plasmid pPS129. We also thank Hayashi Yamamoto, Yukiko Kabeya, Kuninori Suzuki, Hiromi Kirisako, Yoko Hara and the members of our and Fuyuhiko Inagaki's groups for materials, procedures, helpful discussions, and technical and secretarial support. This work was supported in part by grants from the Ministry of Education, Culture, Sports, Science and Technology of Japan.

Supplemental Materials

Supplemental materials can be found at:
www.landesbioscience.com/journals/autophagy/article/18373

References

1. Johnson DR, Bhatnagar RS, Knoll LJ, Gordon JI. Genetic and biochemical studies of protein N-myristoylation. Annu Rev Biochem 1994; 63:869-914; PMID:7979256; http://dx.doi.org/10.1146/annurev.bi.63.070194.004253
2. Linder ME, Deschenes RJ. Palmitoylation: policing protein stability and traffic. Nat Rev Mol Cell Biol 2007; 8:74-84; PMID:17183362; http://dx.doi.org/10.1038/nrm2084
3. Zhang FL, Casey PJ. Protein prenylation: molecular mechanisms and functional consequences. Annu Rev Biochem 1996; 65:241-69; PMID:8811180; http://dx.doi.org/10.1146/annurev.bi.65.070196.001325
4. Nakatogawa H, Suzuki K, Kamada Y, Ohsumi Y. Dynamics and diversity in autophagy mechanisms: lessons from yeast. Nat Rev Mol Cell Biol 2009; 10:458-67; PMID:19491929; http://dx.doi.org/10.1038/nrm2708
5. Yang Z, Klionsky DJ. Eaten alive: a history of macroautophagy. Nat Cell Biol 2010; 12:814-22; PMID:20811353; http://dx.doi.org/10.1038/ncb0910-814
6. Ichimura Y, Kirisako T, Takao T, Satomi Y, Shimonishi Y, Ishihara N, et al. A ubiquitin-like system mediates protein lipidation. Nature 2000; 408:488-92; PMID:11100732; http://dx.doi.org/10.1038/35044114
7. Hanada T, Noda NN, Satomi Y, Ichimura Y, Fujioka Y, Takao T, et al. The Atg12-Atg5 conjugate has a novel E3-like activity for protein lipidation in autophagy. J Biol Chem 2007; 282:37298-302; PMID:17986448; http://dx.doi.org/10.1074/jbc.C700195200
8. Kirisako T, Ichimura Y, Okada H, Kabeya Y, Mizushima N, Yoshimori T, et al. The reversible modification regulates the membrane-binding state of Apg8/Aut7 essential for autophagy and the cytoplasm to vacuole targeting pathway. J Cell Biol 2000; 151:263-76; PMID:11038174; http://dx.doi.org/10.1083/jcb.151.2.263
9. Kim J, Huang WP, Klionsky DJ. Membrane recruitment of Aut7p in the autophagy and cytoplasm to vacuole targeting pathways requires Aut1p, Aut2p, and the autophagy conjugation complex. J Cell Biol 2001; 152:51-64; PMID:11149920; http://dx.doi.org/10.1083/jcb.152.1.51
10. Kirisako T, Baba M, Ishihara N, Miyazawa K, Ohsumi M, Yoshimori T, et al. Formation process of autophagosome is traced with Apg8/Aut7p in yeast. J Cell Biol 1999; 147:435-46; PMID:10525546; http://dx.doi.org/10.1083/jcb.147.2.435
11. Nakatogawa H, Ichimura Y, Ohsumi Y. Atg8, a ubiquitin-like protein required for autophagosome formation, mediates membrane tethering and hemifusion. Cell 2007; 130:165-78; PMID:17632063; http://dx.doi.org/10.1016/j.cell.2007.05.021
12. Suzuki K, Kirisako T, Kamada Y, Mizushima N, Noda T, Ohsumi Y. The pre-autophagosomal structure organized by concerted functions of *APG* genes is essential for autophagosome formation. EMBO J 2001; 20:5971-81; PMID:11689437; http://dx.doi.org/10.1093/emboj/20.21.5971
13. Ichimura Y, Imamura Y, Emoto K, Umeda M, Noda T, Ohsumi Y. In vivo and in vitro reconstitution of Atg8 conjugation essential for autophagy. J Biol Chem 2004; 279:40584-92; PMID:15277523; http://dx.doi.org/10.1074/jbc.M405860200
14. Baba M, Takeshige K, Baba N, Ohsumi Y. Ultrastrucmral analysis of the autophagic process in yeast: Detection of autophagosomes and their characterization. J Cell Biol 1994; 124:903-13; PMID:8132712; http://dx.doi.org/10.1083/jcb.124.6.903
15. Vida TA, Emr SD. A new vital stain for visualizing vacuolar membrane dynamics and endocytosis in yeast. J Cell Biol 1995; 128:779-92; PMID:7533169; http://dx.doi.org/10.1083/jcb.128.5.779
16. Suzuki K, Kubota Y, Sekito T, Ohsumi Y. Hierarchy of Atg proteins in pre-autophagosomal structure organization. Genes Cells 2007; 12:209-18; PMID:17295840; http://dx.doi.org/10.1111/j.1365-2443.2007.01050.x
17. Cao Y, Cheong H, Song H, Klionsky DJ. In vivo reconstitution of autophagy in *Saccharomyces cerevisiae*. J Cell Biol 2008; 182:703-13; PMID:18725539; http://dx.doi.org/10.1083/jcb.200801035
18. Nair U, Cao Y, Xie Z, Klionsky DJ. Roles of the lipid-binding motifs of Atg18 and Atg21 in the cytoplasm to vacuole targeting pathway and autophagy. J Biol Chem 2010; 285:11476-88; PMID:20154084; http://dx.doi.org/10.1074/jbc.M109.080374

19. Xie Z, Nair U, Klionsky DJ. Atg8 controls phagophore expansion during autophagosome formation. Mol Biol Cell 2008; 19:3290-8; PMID:18508918; http://dx.doi.org/10.1091/mbc.E07-12-1292
20. Matsuura A, Tsukada M, Wada Y, Ohsumi Y. Apg1p, a novel protein kinase required for the autophagic process in *Saccharomyces cerevisiae*.. Gene 1997; 192: 245-50; PMID:9224897; http://dx.doi.org/10.1016/S0378-1119(97)00084-X
21. Axe EL, Walker SA, Manifava M, Chandra P, Roderick HL, Habermann A, et al. Autophagosome formation from membrane compartments enriched in phosphatidylinositol 3-phosphate and dynamically connected to the endoplasmic reticulum. J Cell Biol 2008; 182:685-701; PMID:18725538; http://dx.doi.org/10.1083/jcb.200803137
22. Hayashi-Nishino M, Fujita N, Noda T, Yamaguchi A, Yoshimori T, Yamamoto A. A subdomain of the endoplasmic reticulum forms a cradle for autophagosome formation. Nat Cell Biol 2009; 11:1433-7; PMID:19898463; http://dx.doi.org/10.1038/ncb1991
23. Ylä-Anttila P, Vihinen H, Jokitalo E, Eskelinen EL. 3D tomography reveals connections between the phagophore and endoplasmic reticulum. Autophagy 2009; 5:1180-5; PMID:19855179; http://dx.doi.org/10.4161/auto.5.8.10274
24. Matsunaga K, Morita E, Saitoh T, Akira S, Ktistakis NT, Izumi T, et al. Autophagy requires endoplasmic reticulum targeting of the PI3-kinase complex via Atg14L. J Cell Biol 2010; 190:511-21; PMID:20713597; http://dx.doi.org/10.1083/jcb.200911141
25. Itakura E, Mizushima N. Characterization of autophagosome formation site by a hierarchical analysis of mammalian Atg proteins. Autophagy 2010; 6:764-76; PMID:20639694; http://dx.doi.org/10.4161/auto.6.6.12709
26. Satoo K, Noda NN, Kumeta H, Fujioka Y, Mizushima N, Ohsumi Y, et al. The structure of Atg4B-LC3 complex reveals the mechanism of LC3 processing and delipidation during autophagy. EMBO J 2009; 28:1341-50; PMID:19322194; http://dx.doi.org/10.1038/emboj.2009.80
27. Brachmann CB, Davies A, Cost GJ, Caputo E, Li J, Hieter P, et al. Designer deletion strains derived from *Saccharomyces cerevisiae* S288C: a useful set of strains and plasmids for PCR-mediated gene disruption and other applications. Yeast 1998; 14:115-32; PMID:9483801; http://dx.doi.org/10.1002/(SICI)1097-0061(19980130)14:2<115::AID-YEA204>3.0.CO;2-2
28. Adams A, Gottschling DE, Kaiser CA, Stearns T. Methods in Yeast Genetics. New York: Cold Spring Harbor Laboratory Press, 1998.
29. Janke C, Magiera MM, Rathfelder N, Taxis C, Reber S, Maekawa H, et al. A versatile toolbox for PCR-based tagging of yeast genes: new fluorescent proteins, more markers and promoter substitution cassettes. Yeast 2004; 21:947-62; PMID:15334558; http://dx.doi.org/10.1002/yea.1142
30. Strømhaug PE, Reggiori F, Guan J, Wang CW, Klionsky DJ. Atg21 is a phosphoinositide binding protein required for efficient lipidation and localization of Atg8 during uptake of aminopeptidase I by selective autophagy. Mol Biol Cell 2004; 15:3553-66; PMID:15155809; http://dx.doi.org/10.1091/mbc.E04-02-0147
31. Noda T, Matsuura A, Wada Y, Ohsumi Y. Novel system for monitoring autophagy in the yeast *Saccharomyces cerevisiae*.. Biochem Biophys Res Commun 1995; 210: 126-32; PMID:7741731; http://dx.doi.org/10.1006/bbrc.1995.1636